13th International Conference on Greenhouse Gas Control Technologies, GHGT-13, 14-18 November 2016, Lausanne, Switzerland

Process modelling and simulation of degradation of 2-amino-2-methyl-1-propanol (AMP) capture plant

Ebuwa Osagie[a], Chechet Biliyok[b], Giuseppina Di Lorenzo[c], Vasilije Manovic[a], *

[a]Combustion and CCS Centre, Cranfield University, Bedfordshire MK43 0AL, UK

Abstract

The presence of contaminants in the flue gas stream such as O_2, CO_2, SO_X, and NO_X can cause solvent degradation in solvent-based CO_2 capture processes. In this study, the major degradation products reactions of the AMP-based CO_2 capture process has been included in the Aspen Plus® V8.4 simulation software using equilibrium reactions. Assessing the solvent degradation, solvent concentration and flowrate were varied. The results showed that the AMP losses reduced by decreasing solvent flowrate and concentration. Largest energy savings are observed when increasing concentration up to 34 wt. %.

1. Introduction

Amine degradation occurs with the prolonged use of solvents mostly in the oxidative environment, which transforms into products that cannot easily be regenerated. These degradation products then react with amines to form heat stable salts, which accumulate in the system over time. The problems associated with degradation include decreased plant equipment life, foaming, corrosion, high solution viscosity, and diminished acid gas removal capacity. Amines generally pose lots of emission risk. Researchers have therefore taken interests in the characterization and quantification of atmospheric emissions of amines and their degradation products. Hence, identification of the operating conditions that lead to the degradation of the amines, the concentrations, and the nature of the degradation products formed will be important.

Unlike other solvents such as MEA, the interaction between AMP and O_2 has not been widely explored. In general, there is limited information regarding oxidative degradation of AMP. Lots of studies have considered

oxidative degradation of MEA and both experimental and simulations models have been investigated [1], [2], [3], [4]. While for the AMP oxidative degradation, few authors [5], [6], [7], [8], [9] have carried out experimental studies to determine the degradation products for AMP, no simulation model for AMP oxidative degradation developed. In this study, the major degradation products of AMP are simulated and modelled with equilibrium reactions using Aspen Plus® simulation software. Process operating conditions such as solvent concentration and flowrate were varied to assess the solvent degradation.

Nomenclature	
AMP	2-amino-2-methyl-1-propanol
MEA	Monoethanolamine
CCS	Carbon capture and storage
PCC	Post-combustion capture
DMOZD	4, 4-dimethyl-2-oxazolidinone
DGAQFM	Gibbs free energy of formation
NRTL	Non-random two liquid

_____

* Corresponding author. Tel.: +44(0)1234 754649; fax: +44 1234751671.
  E-mail address: v.manovic@cranfield.ac.uk (V. Manovic).

2. AMP Degradation Chemistry

2.1. Mechanism for the degradation products

Reaction mechanisms and reaction pathways give useful information about the degradation phenomena present in the absorption chemistry of CO_2 in amine solvents. Two mechanisms are likely to occur; electron abstraction and hydrogen abstraction. The mechanism involved at the initial step in the formation of these AMP degradation products is the hydrogen abstraction [5]. The proposed oxidative pathways for AMP, these are shown below;

A major product observed in the thermally degraded AMP aqueous solutions was 4, 4-dimethyl-2-oxazolidinone (DMOZD).
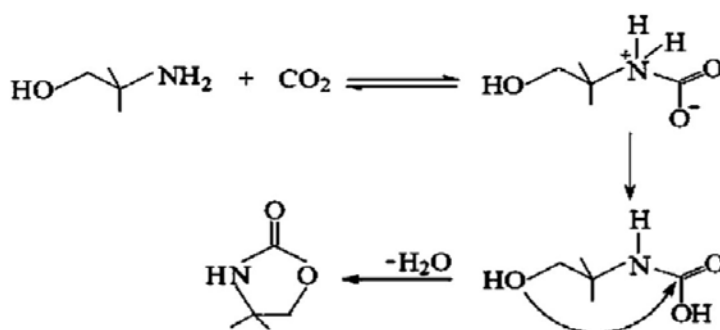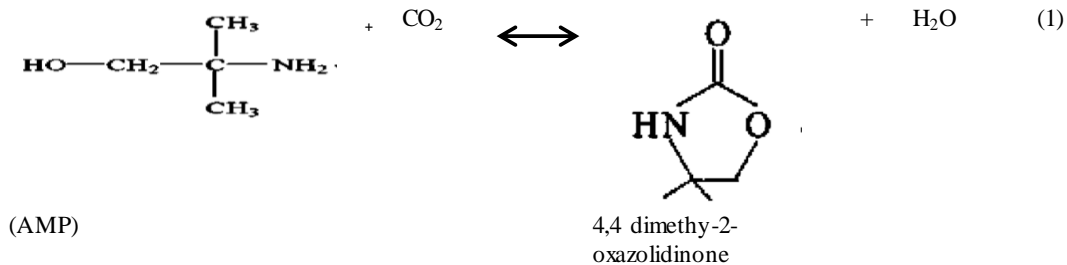

Fig. 1. Scheme for degradation of AMP with CO_2 [5]

The stoichiometric coefficients of the degradation products are determined by eliminating the intermediates and

the equation is balanced as follows;

(AMP)   4,4 dimethy-2-
                                                     oxazolidinone

2.2. Formation of 2,4-Lutidine

A major oxidative degradation product of AMP is 2, 4-Lutidine. This involves the reaction formaldehyde and an imine to form 2, 4-Lutidine.
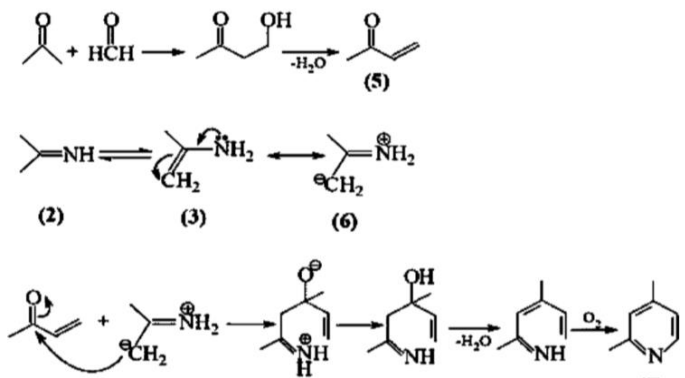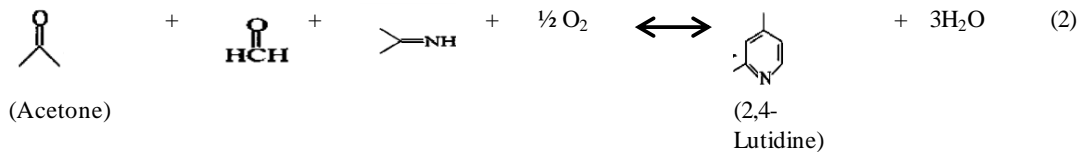

Fig. 2. Formation of 2, 4-Lutidine [5]

Eliminating the intermediates, the reaction is as follows;

(Acetone)   (2,4-
                                                     Lutidine)

2.3. Formation of Acetone

The final oxidative degradative product of AMP is Acetone.
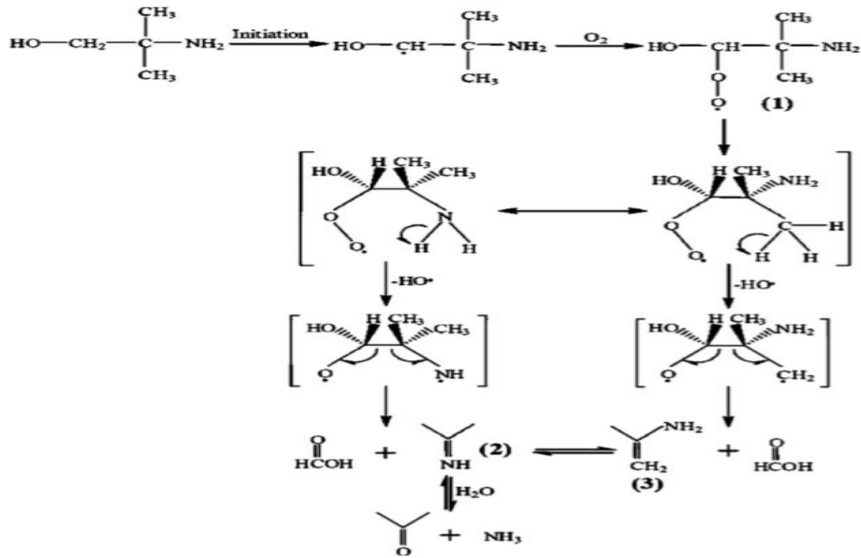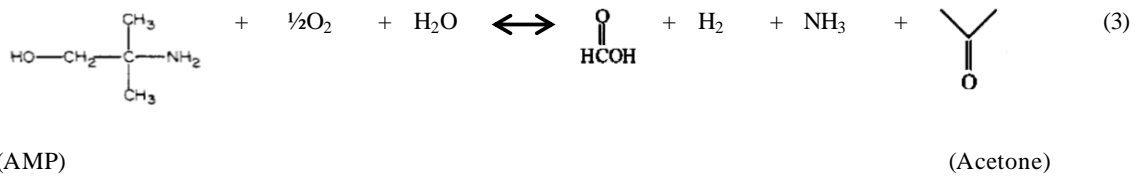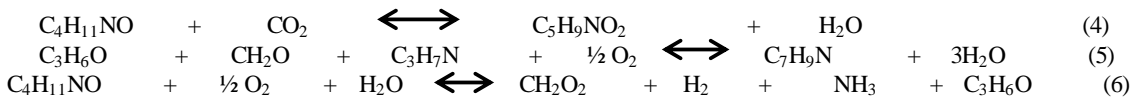
Fig. 3. Scheme for degradation of AMP with O_2 [5]

Eliminating the intermediates, the reaction is as follows;

(3)

(AMP)   (Acetone)

2.4. Design approach of degradation reactions in Aspen Plus

The major degradation products of AMP identified between temperatures 100 – 140 ^{o} C, initial AMP concentration, 5 mol/kg, at 250 kPa O_2 are acetone, 2, 4-lutidine and 4,4 dimethyl-2-oxazolidinone (DMOZD) [5]. These three degradation products reactions have been included into a global process validated model built in Aspen Plus® V 8.4. The degradation products modelled with equilibrium reactions are applied to the steady state modelling of the absorption process because in describing small-scale changes over time, dynamic simulations are not suitable [10]. In addition, the component data for the degradation reactions; acetone and 4,4 dimethy-2-oxazolidinone were retrieved from Aspen Plus® databases, while 2,4 Lutidine had no data available but was estimated by Aspen Plus® based on molecular structure and weight. The equilibrium constants (K_{eq}) for the reactions presented in equations (1) – (3) are calculated from Gibb's free energy change ($\Delta G = $ -RT ln K). Gibbs free energy of formation (DGAQFM); an inbuilt correlation in Aspen plus, is used in the estimation of Gibbs free energy using the empirical relation developed by Aspen Technology [11].

The equilibrium equations which describes the chemistry are defined by equations (4) – (6)

$$C_4H_{11}NO + CO_2 \longleftrightarrow C_5H_9NO_2 + H_2O \qquad (4)$$
$$C_3H_6O + CH_2O + C_3H_7N + \frac{1}{2}O_2 \longleftrightarrow C_7H_9N + 3H_2O \qquad (5)$$
$$C_4H_{11}NO + \frac{1}{2}O_2 + H_2O \longleftrightarrow CH_2O_2 + H_2 + NH_3 + C_3H_6O \qquad (6)$$

3. Modelling Framework
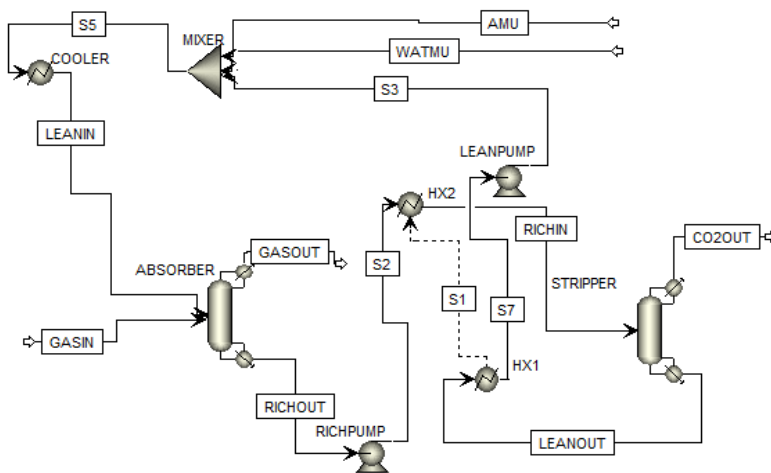
3.1. Model description

Fig. 4. Process flowsheet of AMP capture plant

Fig. 4. shows a screenshot of the AMP capture plant. The design of absorber and stripper columns is well described in the literature [12]. The model adopted for the thermodynamic properties is based on the work by [13]. The electrolyte NRTL model is used to describe the liquid phase thermodynamic state, while the Redlich-Kwong equation of state used for the vapour phase. The process is a steady state process which consists of two columns; (an absorber and a stripper), a cross heat exchanger represented by two heaters, a cooler and two pumps, connected in a closed cycle to achieve good prediction of the performance of the process [14]. Rich AMP exiting the bottom of the absorber is pumped to the cross exchanger, and exchanges heat with the lean solvent exiting the reboiler before entering the stripper. This lean solvent from the stripper is pumped and further cooled to 40 $^{\mathrm{o}}$ C before it is sent to the absorber. The stripper (regenerator) operates at a moderately high pressure of 1.95 bar. The flowsheet also consists of water and AMP make-up systems; this is important in order to keep a water balance in the plant and to ensure robust convergence of the model.

3.2. Model validation at pilot scale

The model is validated with experimental studies using data reported by Gabrielsen et al. [15], presented in Table 1 and compared with one experimental case study. Experimental run 'R4' out of the eleven runs in the experimental studies was chosen for comparison with simulated results. Further validation analysis with more experimental data points has been carried out by Osagie et al. (To be submitted). Design parameters of the experimental pilot plant are given in Table 1.

Table 1. Design data of the pilot plant [15]

	Absorber	Stripper
Diameter (m)	0.15	0.10
Packing height (m)	4.36	3.89
Packing	Sulzer Mellapak 250Y	Sulzer Mellapak 250Y
Type of packing	Structured	Structured

3.3. Absorber model validation

From Table 2, it is clear that the closest prediction by the three different sets of mass transfer correlations is the Billet and Schultes correlation [16]. The model predictions and pilot plant data differ by less than 7% for capture level and rich loading when using the Billet and Schultes correlation [16]

Fig. 5. shows the comparison of temperature profiles in the absorber. The figures clearly show that the model predictions are in agreement with the experimental data for all three different sets of mass transfer correlations, specifically showing the correct trend and the temperature bulge in the column. This bulge is dependent on the L/G ratio and shows the location where CO_2 absorption into AMP is concentrated in the column, which results in the large release of heat of reaction [17]. It is clear from the location of the bulge that Case 4 has a low L/G ratio. Some deviations from the model prediction to the pilot plant data remain, and these deviations increase for all three sets of mass transfer correlations with increasing L/G ratio. In addition, the model underestimates the temperatures in the absorber, yet the predictions for the Billet and Schultes correlation [16] is consistently closer to the pilot plant data. In conclusion, the Billet and Schultes [16], correlations provide absorber temperature profiles that are very close to the pilot plant data, and therefore, could be used for further process analysis.

Table 2. Comparison of absorber model prediction with experimental data

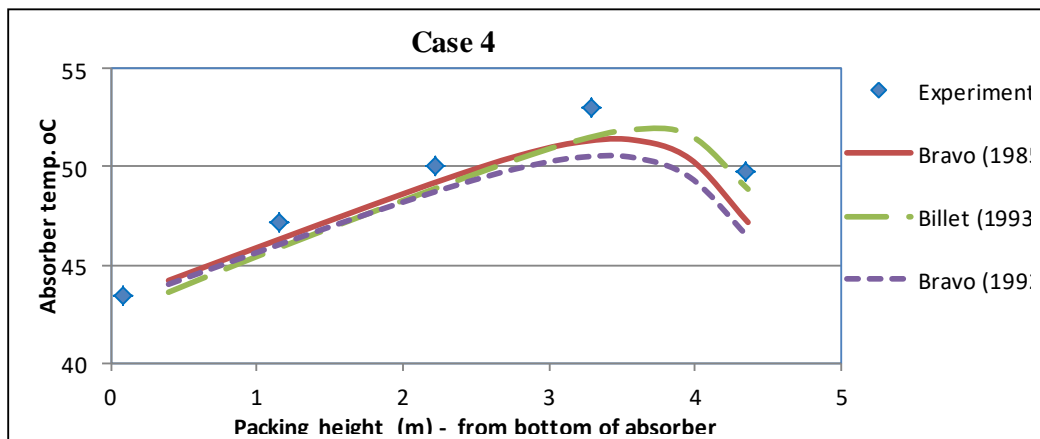|	Rich Loading (mol/mol)			Capture level (%)		
	Case 4					
	Exp	Model	% diff.	Exp	Model	% diff.
Bravo (1985)	0.379	0.403	5.96	29.85	24.79	16.95
Billet and Schultes (1993)	0.379	0.404	6.10	29.85	28.81	3.48
Bravo (1992)	0.379	0.368	2.90	29.85	24.05	19.43

Fig. 5. Temperature profile of absorber

3.4. Stripper model validation

From Table 3, the model predictions closely match the pilot plant data for all three sets of mass transfer correlations. The Bravo 1985 correlations [18] and Bravo 1992 correlations [19], provide similar predictions and the closest match to pilot plant.

Fig. 6. shows the temperature profiles present in the stripper for case 4. The predictions for all three sets of mass transfer correlations are largely indistinguishable from each other and match the pilot plant data. In fact, the pilot plant data and model gave similar L-shape curves, to be expected; in a stripper, thus confirming that the model can be relied upon for further process analysis.

Table 3. Comparison of stripper model prediction with experimental data

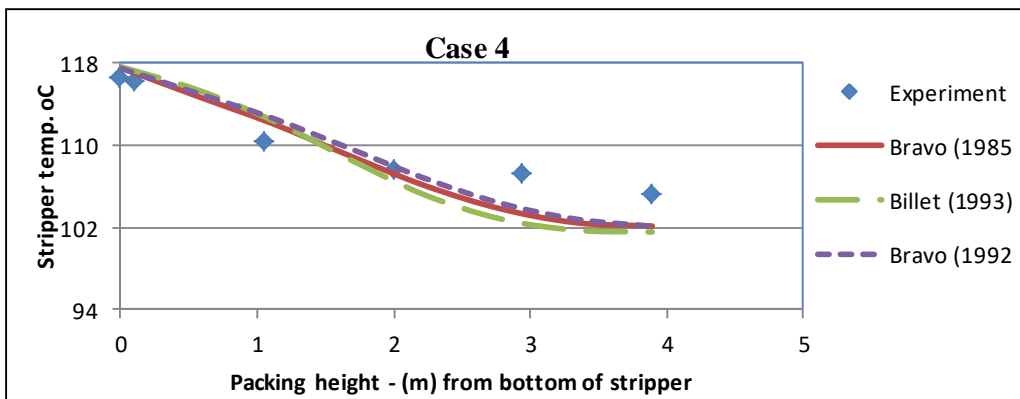|	Lean out (mol/mol)			Reboiler temperature (°C)		
	Case 4					
	Exp	Model	% diff.	Exp	Model	% diff.
Bravo (1985	0.118	0.120	1.7	116.6	117.66	0.9
Billet and Schultes (1993)	0.118	0.115	2.6	116.6	117.77	1.0
Bravo (1992)	0.118	0.121	2.5	116.6	117.63	0.9

Fig. 6. Temperature profile of stripper

4. Impact of process variables on solvent degradation

These are key parameters in the design of the CO_2 capture plant

- Solvent flowrate
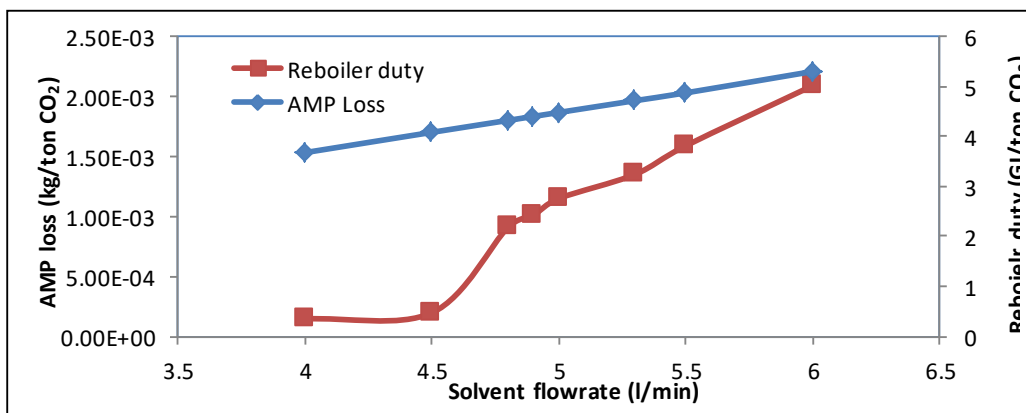- Solvent concentration

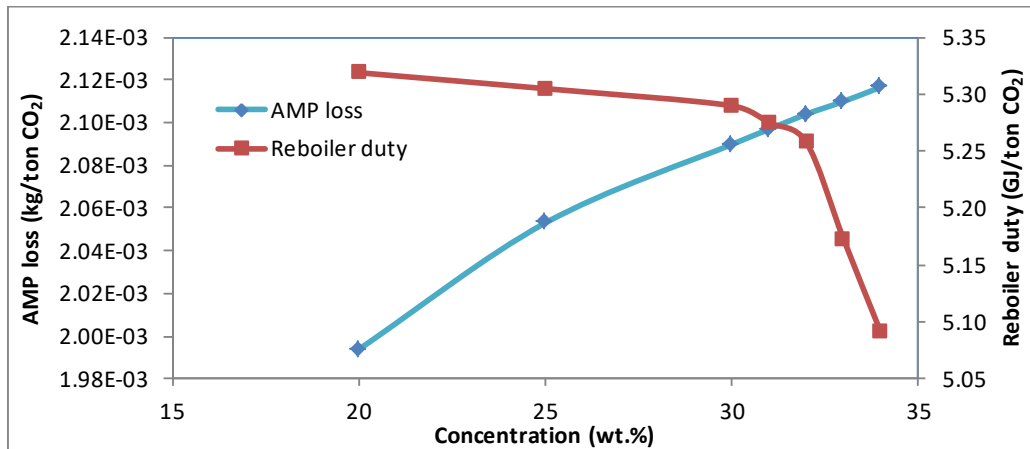Fig. 7. Effect of solvent flow rate on AMP loss and reboiler duty

Fig. 8. Effect of solvent concentration on AMP loss and reboiler duty

Table 4. Degradation for base case

Parameters	Unit	Absorber	Stripper	Total
AMP degradation	kg/tons CO_2	2.09E-03	8.10E-04	2.81E-03
Acetone	kg/tons CO_2	1.34E-06	1.36E-06	2.70E-06
4-oxazolidinone formation	kg/tons CO_2	2.70E-06	2.65E-06	5.35E-06
2,4 Lutidine	kg/tons CO_2	4.24E-04	2.29E-06	4.26E-04
AMP emission	kg/tons CO_2	1.25E-03	2.45E-06	1.25E-03
Acetone	kg/tons CO_2	7.88E-09	1.70E-15	7.88E-09
4-oxazolidinone emission	kg/tons CO_2	1.56E-08	3.37E-15	1.56E-08
2,4 Lutidine	kg/tons CO_2	1.11E-05	1.90E-08	1.11E-05

As shown in Table 4, degradation mainly takes place in the absorber, thus oxidative degradation is more important that thermal degradation [5]. Total AMP degradation is 2.81E-03 kg/t CO_2 for a solvent flowrate of 6 Litres/min (0.36 m^3/hr), which is equivalent to 2.9E-03 kg AMP/day; while the emissions obtained is 1.25E-03 kg/t CO_2. A previous study [10] has reported MEA degradation using a small-scale plant to be 0.081 kg/t CO_2 for a solvent flowrate of 24 m^3/hr. Results from this study have shown that the amine losses for the small-scale capture plant are higher for AMP than MEA, a reason for this could be the molecular structure and properties of AMP which leads to a high volatility of AMP [20]. These results obtained from small-scale plants can be considered insignificant when compared to that for large-scale degradation which is 324 kg MEA/day [10]. As reported from experimental studies [5], 2,4, Lutidine is the main emitted degradation product from the absorber.

Fig. 7. and Fig. 8. shows the effect of solvent concentration and solvent flowrate on solvent loss and energy required for regeneration. The same capture level, approximately 30%, present at the pilot plant, was maintained to

carry out the sensitivity studies. Results showed that solvent flowrate increases with AMP loss and reboiler duty, this is expected since as the amount and concentration of AMP increases, it creates more opportunity for the solvent to be lost and also more energy will be required. Also, as AMP concentration increases from 30 wt. % to 34 wt. %; a 5% reduction in reboiler duty is attained, below 30 wt. %, no significant reductions observed. However, this increase in concentration above 30 wt. % causes a slight increase (below 1%) in AMP loss, while below 30 wt. % about 3% increment in AMP losses is achieved. Thus, very low and very high concentrations are not desirable. Finally, reboiler duty decreases with increase in concentration because the water (wt. %) in the solvent decreases, thus, water heat of vaporisation will be very high, so the reduced water content decrease reboiler duty.

5. Conclusion

The assessment of AMP degradation and energy requirement has been carried out. AMP degradation reactions were included into the Aspen Plus® process model to study the impact of process variables. Results showed that the oxidative degradation of AMP at small scale was 2.9E-03 kg AMP/day; this compared to large-scale for MEA is very low. Thus, the amine emissions into the atmosphere are most significant when considering a large-scale post-combustion CO_2 emission reduction from power plants. Therefore, a simulation study on large-scale analysis is required. The process variables have shown to have an impact on the solvent loss and energy required for regeneration, thus, identification of the best operating points is important. Further modelling studies may consider the kinetics of the degradation products.

References

1. Bello A, Idem RO. Comprehensive study of the kinetics of the oxidative degradation of CO_2 loaded and concentrated aqueous monoethanolamine (MEA) with and without sodium metavanadate during CO_2 absorption from flue gases. Industrial and Engineering Chemistry Research. 2006; 45(8): 2569–2579. Available at: DOI:10.1021/ie050562x

2. Supap T, Idem R, Tontiwachwuthikul P, Saiwan C. Analysis of monoethanolamine and its oxidative degradation products during CO_2 absorption from flue gases: A comparative study of GC-MS, HPLC-RID, and CE-DAD analytical techniques and possible optimum combinations. Industrial and Engineering Chemistry Research. 2006; 45(8): 2437–2451. Available at: DOI:10.1021/ie050559d

3. Vevelstad SJ, Eide-Haugmo I, Da Silva EF, Svendsen HF. Degradation of MEA; A theoretical study. Energy Procedia. Elsevier; 2011; 4: 1608–1615. Available at: DOI:10.1016/j.egypro.2011.02.031

4. Goff GS, Rochelle GT. Monoethanolamine Degradation: O_2 Mass Transfer Effects under CO_2 Capture Conditions. Industrial & Engineering Chemistry Research. 2004; 43(20): 6400–6408. Available at: DOI:10.1021/ie0400245

5. Wang T, Jens KJ. Oxidative degradation of aqueous 2-amino-2-methyl-1-propanol solvent for post combustion CO_2 capture. Industrial and Engineering Chemistry Research. 2012; 51: 6529–6536. Available at: DOI:10.1021/ie300346j

6. Wang T, Jens K-J. Oxidative Degradation of AMP/MEA Blends for Post-combustion CO2 Capture. Energy Procedia. Elsevier B.V.; 2013; 37(1876): 306–313. Available at: DOI:10.1016/j.egypro.2013.05.116

7. Jeon S, Lee S, Kang M, Oh K-J. Characteristics of Absorbent Loss and CO_2-Selective Absorption of CO_2/SO_2 Gas into Aqueous 2-Amino-2-methyl-1-propanol/Ammonia Solution. Industrial & Engineering …. 2013; : 4881–4887. Available at: http://pubs.acs.org/doi/full/10.1021/ie302667z

8. Wang T, Jens K-J. Oxidative degradation of aqueous PZ solution and AMP/PZ blends for post-combustion carbon dioxide capture. International Journal of Greenhouse Gas Control. 2014; 24: 98–105. Available at: DOI:10.1016/j.ijggc.2014.03.003

9.   Wang T, Jens K-J. Towards an understanding of the oxidative degradation pathways of AMP for post-combustion CO2 capture. International Journal of Greenhouse Gas Control. 2015; 37: 354–361. Available at: DOI:10.1016/j.ijggc.2015.03.017

10.   Gregoire Leonard, Dominique Toye GH. Assessment of Solvent Degradation within Global Process Model of Post-Combustion CO2 capture. 24th European Symposium on Computer Aided Process Engineering. Hungary: Elservier; 2014.

11.   Aspen Technology I. Aspen Plus® User Guide. Aspen Technology, Inc. 2000; p: 936.

12.   Aspen Technology I. Rate-Based Model of the CO2 Capture Process by AMP using Aspen Plus. 2008. *Aspen Technology, Inc*, Cambridge, MA, USA.

13.   Austgen DM, Rochelle GT, Chen CC, Peng X. Model of vapor-liquid equilibria for aqueous acid gas-alkanol amine systems using the electrolyte-NRTL equation. Industrial & Engineering Chemistry Research. 1989; 28(7): 1060–1073. Available at: DOI:10.1021/ie00091a028

14.   Biliyok C, Yeung H. International Journal of Greenhouse Gas Control Evaluation of natural gas combined cycle power plant for post-combustion CO_2 capture integration. International Journal of Greenhouse Gas Control. Elsevier Ltd; 2013; 19: 396–405. Available at: DOI:10.1016/j.ijggc.2013.10.003

15.   Gabrielsen J, Svendsen HF, Michelsen ML, Stenby EH, Kontogeorgis GM. Experimental validation of a rate-based model for CO_2 capture using an AMP solution. Chemical Engineering Science. 2007; 62(9): 2397–2413. Available at: DOI:10.1016/j.ces.2007.01.034

16.   Billet PD-IR, Schultes D-IM. Predicting mass transfer in packed columns. Chemical Engineering & Technology. 1993; 16(1 February): 1–9.

17.   Kvamsdal HM, Rochelle GT. Effects of the temperature bulge in CO_2 absorption from flue gas by aqueous monoethanolamine. Industrial and Engineering Chemistry Research. 2008; 47(3): 867–875. Available at: DOI:10.1021/ie061651s

18.   Bravo JL, Rocha JA FJ. Mass transfer in gauze packings. Hydrocarbon Processing. 1985; : 64(1):91–95.

19.   Bravo, Jose L., J. Antonio Rocha and JRF. 'A comprehensive model for the performance of columns containing structured packings.' Institution of Chemical Engineers Symposium Series. Vol. 128. HEMISPHERE PUBLISHING CORPORATION, 1992;

20.   Nguyen T, Hilliard M, Rochelle GT. Amine volatility in CO_2 capture. International Journal of Greenhouse Gas Control. Elsevier Ltd; 2010; 4(5): 707–715. Available at: DOI:10.1016/j.ijggc.2010.06.003